



# Dda Helicase Tightly Couples Translocation on Single-Stranded DNA to Unwinding of Duplex DNA: Dda Is an Optimally Active Helicase

Alicia K. Byrd<sup>1</sup>, Dennis L. Matlock<sup>2</sup>, Debjani Bagchi<sup>3</sup>,  
Suja Aarattuthodiyil<sup>1</sup>, David Harrison<sup>1</sup>, Vincent Croquette<sup>3\*</sup>  
and Kevin D. Raney<sup>1\*</sup>

<sup>1</sup>Department of Biochemistry and Molecular Biology, University of Arkansas for Medical Sciences, 4301 West Markham Street, Slot 516, Little Rock, AR 72205, USA

<sup>2</sup>Department of Chemistry, Harding University, 915 East Market Avenue, Searcy, AR 72143, USA

<sup>3</sup>Laboratoire de Physique Statistique and IBENS, Ecole Normale Supérieure, UPMC Université Paris 06, Université Paris 11 Diderot, CNRS, 24 Rue Lhomond, 75005 Paris, France

Received 4 January 2012;  
received in revised form  
4 March 2012;  
accepted 1 April 2012  
Available online  
11 April 2012

Edited by J. Berger

**Keywords:**  
molecular motor;  
single-molecule;  
stopped-flow;  
DNA;  
fluorescence

Helicases utilize the energy of ATP hydrolysis to unwind double-stranded DNA while translocating on the DNA. Mechanisms for melting the duplex have been characterized as active or passive, depending on whether the enzyme actively separates the base pairs or simply sequesters single-stranded DNA (ssDNA) that forms due to thermal fraying. Here, we show that Dda translocates unidirectionally on ssDNA at the same rate at which it unwinds double-stranded DNA in both ensemble and single-molecule experiments. Further, the unwinding rate is largely insensitive to the duplex stability and to the applied force. Thus, Dda transduces all of its translocase activity into DNA unwinding activity so that the rate of unwinding is limited by the rate of translocation and that the enzyme actively separates the duplex. Active and passive helicases have been characterized by dividing the velocity of DNA unwinding in base pairs per second ( $V_{un}$ ) by the velocity of translocation on ssDNA in nucleotides per second ( $V_{trans}$ ). If the resulting fraction is 0.25, then a helicase is considered to be at the lower end of the “active” range. In the case of Dda, the average DNA unwinding velocity was  $257 \pm 42$  bp/s, and the average translocation velocity was  $267 \pm 15$  nt/s. The  $V_{un}/V_{trans}$  value of 0.96 places Dda in a unique category of being an essentially “perfectly” active helicase.

© 2012 Elsevier Ltd. All rights reserved.

## Introduction

Helicases are enzymes that unwind double-stranded DNA (dsDNA) to provide the single-stranded DNA (ssDNA) intermediates necessary for virtually every phase of nucleic acid (NA) metabolism, reviewed in Refs. 1–3. They are ubiquitous, and most organisms encode multiple helicases for involvement in different cellular processes. Canonical helicases use the energy of

\*Corresponding authors. E-mail addresses: [vincent.croquette@lps.ens.fr](mailto:vincent.croquette@lps.ens.fr); [raneykevind@uams.edu](mailto:raneykevind@uams.edu).

Abbreviations used: dsDNA, double-stranded DNA; ssDNA, single-stranded DNA; NA, nucleic acid; dsNA, double-stranded nucleic acid.

NTP hydrolysis to fuel unidirectional translocation on NAs and concomitant unwinding of duplex NA.

Whether the helicase physically interacts with and melts the double-stranded nucleic acid (dsNA), an active mechanism, or whether the helicase traps partially melted NA, a passive mechanism, is a fundamental characteristic of helicase-catalyzed NA unwinding.<sup>4</sup> In an active mechanism, the helicase physically interacts with the dsNA resulting in unzipping of the duplex. For a passive helicase, the activation energy required to unwind dsNA is high, resulting in the rate-limiting step being unwinding. Therefore, the ratio between unwinding and translocation rates can be used to determine whether a helicase is active or passive.<sup>5</sup> An active helicase will unwind dsDNA and translocate on ssDNA at similar rates. A passive helicase will display a lower rate for unwinding than translocation; of course, a helicase may display intermediate behavior that can be quantified by the strength of the destabilizing energy melting the DNA. Since increasing the GC content of a duplex increases the activation energy required only if unwinding is rate limiting, comparison of the rates of unwinding with high and low GC content duplexes can be used to determine whether a helicase is active or passive. For a passive helicase, the unwinding rate will decrease with increasing GC content in the NA.

Dda is a helicase from bacteriophage T4 involved in early events in DNA replication.<sup>6</sup> It is not essential for growth of the phage but is involved in origin-dependent replication and aids in recombination by increasing the rate of branch migration catalyzed by the T4 recombinase UvsX.<sup>7</sup> It has been suggested to translocate unidirectionally, but the rate of translocation has not been measured. Jongeneel *et al.* investigated the directionality of translocation using partially duplex DNA substrates with either a 3'-ssDNA or a 5'-ssDNA adjacent to the duplex.<sup>8</sup> Dda could unwind substrates with a 5'-ssDNA overhang but not a 3'-ssDNA overhang, suggesting 5'-to-3' translocation. Raney and Benkovic studied the effect of a streptavidin block on the kinetics of ATP hydrolysis by Dda.<sup>9</sup> A 5'-streptavidin block had no effect on the ATPase kinetics while a 3'-streptavidin block reduced the  $K_m$  for DNA, suggesting translocation in the 5'-to-3' direction. Morris and Raney showed that Dda is able to displace streptavidin from 3'-biotinylated oligonucleotides but not from 5'-biotinylated oligonucleotides, again suggesting translocation in the 5'-to-3' direction.<sup>10</sup> The kinetics of unwinding and protein displacement by Dda have been extensively studied. Dda does not form stable oligomers<sup>11</sup> and has been shown to unwind DNA as a monomer,<sup>12</sup> albeit with low processivity.<sup>13</sup> The processivity increases when multiple Dda molecules are bound to the substrate,<sup>14</sup> although the rate of unwinding remains similar.<sup>13</sup>

Dda displaces proteins from ssDNA<sup>10,15</sup> and from dsDNA.<sup>16</sup> Dda interacts primarily with the translocation strand;<sup>17</sup> however, it also appears to interact with the displaced strand during specific steps of the unwinding mechanism.<sup>18</sup>

In this report, we determined the kinetics of Dda's interactions with ssDNA. We show that the unidirectional translocation rate on ssDNA is very similar to the rate of unwinding of dsDNA, indicating that Dda is an active helicase. This is further supported by the result that Dda is insensitive to the GC content of short duplexes during unwinding and to the applied force during unwinding under single-molecule conditions.

## Results

### Dda associates with DNA at near-diffusion-controlled rates

For Dda helicase, the rate of unwinding<sup>13,18</sup> and protein displacement<sup>10,15,16</sup> and the equilibrium binding constants for various DNA substrates<sup>11,12,14</sup> have been well studied. However, the rates at which Dda binds to, dissociates from, and translocates on ssDNA have not been investigated.

When Dda is rapidly mixed with ssDNA, the fluorescence change in tryptophan is biphasic and can be fit with a double exponential as shown in Fig. 1a. The second phase of the reaction is independent of the concentration of DNA, while the rate of the first phase increases as the DNA concentration increases, indicating that the first phase is association of DNA and Dda (Table S1). The slower second phase likely represents a slow isomerization. The rates of Dda association with increasing concentrations of poly(dT) are plotted in Fig. 1b. The second-order association constant obtained from the slope of the line is  $1.66 \times 10^8 \text{ M}^{-1} \text{ s}^{-1}$ , which indicates that this rate is close to diffusion controlled ( $10^8$ – $10^9 \text{ M}^{-1} \text{ s}^{-1}$ ).

### Measurement of the rate constant for Dda dissociation from circular DNA

In order to determine the spontaneous dissociation rate constant in both the presence and the absence of ATP, and therefore the effect of ATP binding and hydrolysis on dissociation, we used a circular DNA species. This prevents Dda from translocating off the end of an oligonucleotide and affecting the observed dissociation rate constant. The fluorescence of Dda is significantly different when bound to DNA *versus* heparin; thus, heparin serves an effective trap (Fig. S1). Dda was pre-incubated with M13 ssDNA and rapidly mixed with heparin in the absence (Fig. 2a) or presence (Fig. 2b) of ATP. The rapid fluorescence increase is

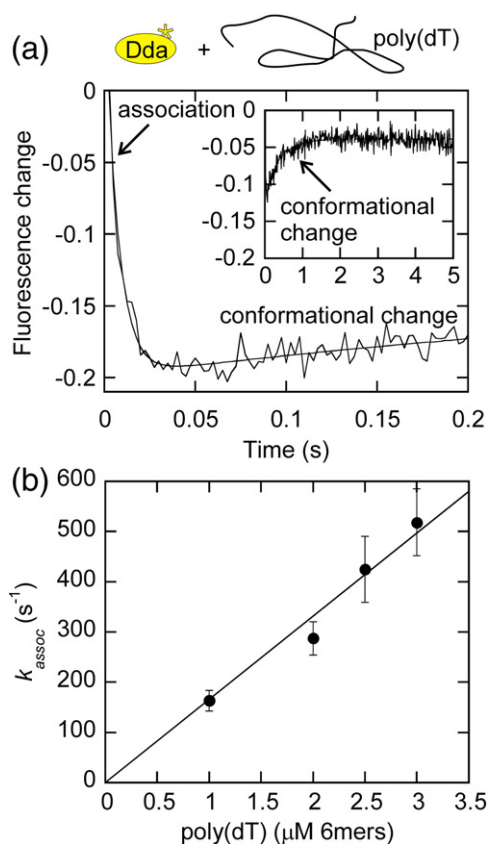


**Fig. 1.** Measurement of the rate of Dda association with DNA. (a) The fluorescence change for 200 nM Dda association with 6  $\mu\text{M}$  poly(dT), in nucleotides, is plotted. Data were fit to a double exponential. The observed rate of association (first phase) is  $163 \pm 20 \text{ s}^{-1}$  at 6  $\mu\text{M}$  poly(dT), in nucleotides [1  $\mu\text{M}$  poly(dT), in binding sites]. The second phase (shown in inset) remains constant as the poly(dT) concentration increases (Table S1) and likely represents a slow conformational change. (b) The rate of association (first phase) increases linearly with increasing poly(dT) concentration. Data were plotted with the poly(dT) concentration in 6mers since Dda is known to have a 6-nt binding site size<sup>15</sup> and was fit to a line using KaleidaGraph software. The slope of the line,  $1.66 \times 10^8 \text{ M}^{-1} \text{ s}^{-1}$ , represents the association rate constant.

dependent only on the presence of DNA (Table S2), suggesting that it represents dissociation of Dda from DNA. The fluorescence change was fit to a single exponential. Dda dissociates from circular DNA at  $1.12 \pm 0.04 \text{ s}^{-1}$  in the absence of ATP and at  $1.94 \pm 0.03 \text{ s}^{-1}$  in the presence of ATP. This suggests that the binding and hydrolysis of ATP causes only a slight increase in the rate constant for dissociation from internal sites on ssDNA. The dissociation rate was independent of the heparin concentration, indicating that heparin binds to Dda rapidly and that the concentration of heparin used is sufficiently high for the rate to be independent of heparin concentration (Table S2).

### Measurement of the rate constant for Dda dissociation from varying length oligonucleotides

In the presence of ATP, the dissociation rate constant decreases as the length of the DNA increases (Fig. 3a). The rate constants are faster for oligonucleotides than for circular DNA and increase as the length of the substrate decreases, presumably due to translocation off the end of the substrate. As the length of the oligonucleotide increases, the helicase has a longer distance to translocate, assuming that Dda binds randomly to each substrate. Since the dissociation rate constant is inversely proportional to the length of the oligonucleotide [Eq. (1)], translocation is unidirectional, and the velocity of translocation on ssDNA ( $V_{\text{trans}}$ ) is equal to one-half the inverse slope of the  $1/k_{\text{d-end}}$  versus  $L-4$  plot (Fig. 3b). Dda dissociation from linear DNA is faster in the presence of ATP than in the absence of ATP due to translocation off the end of the oligonucleotide (Fig. S2). For very short oligonucleotides that are close to the length of the binding site size (6 nt),<sup>15</sup> the relationship between the dissociation rate constant and the DNA length is nonlinear. The ends of

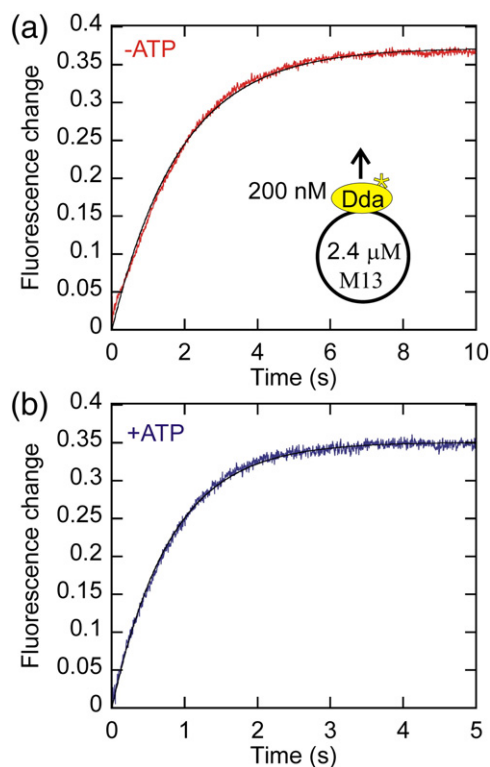


**Fig. 2.** Measurement of the dissociation rate constant for Dda from circular DNA. The intrinsic dissociation of Dda (200 nM) from M13 ssDNA (2.4  $\mu\text{M}$ , in nucleotides) was measured in the absence (a) and in the presence (b) of ATP by rapidly mixing with heparin. The obtained dissociation rate constants were  $1.12 \pm 0.04 \text{ s}^{-1}$  in the absence of ATP and  $1.94 \pm 0.03 \text{ s}^{-1}$  in the presence of ATP.

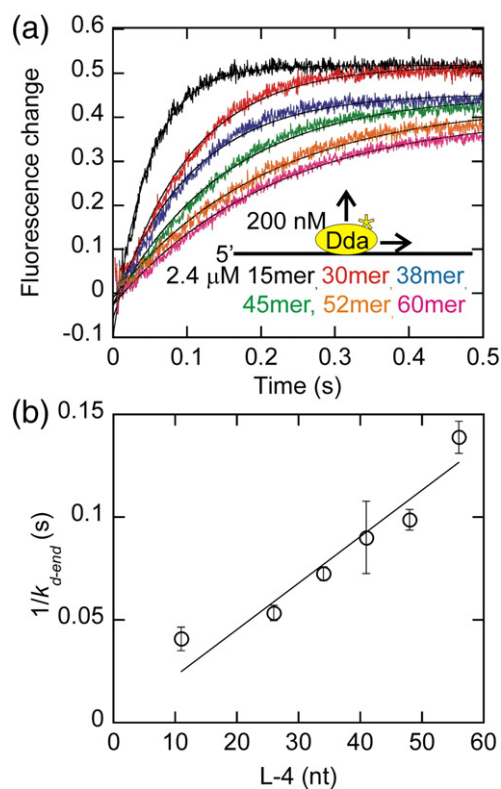


**Fig. 3.** Measurement of the rate constant for dissociation of Dda from oligonucleotides of increasing length. (a) The change in fluorescence of Dda (200 nM) as it dissociates from 2.4  $\mu$ M oligonucleotide of increasing length in the presence of ATP is plotted. The rate constants obtained from single-exponential fits were  $26.3 \pm 1.1$  s $^{-1}$ ,  $22.6 \pm 1.8$  s $^{-1}$ ,  $16.4 \pm 0.8$  s $^{-1}$ ,  $13.6 \pm 2.8$  s $^{-1}$ ,  $12.1 \pm 0.6$  s $^{-1}$ , and  $8.7 \pm 0.4$  s $^{-1}$  for dissociation from the 15mer, 30mer, 38mer, 45mer, 52mer, and 60mer, respectively. (b) The inverse of the rate constant for dissociation from the end of the oligonucleotide,  $k_{d-end}$ , is plotted versus the length of the substrate, adjusted for binding site size. Only oligonucleotides of at least 30 nt in length are included in the fit. One-half the inverse slope of the resulting line provides a velocity of translocation by Dda of  $252 \pm 11$  nt/s. The fit was constrained through the origin to constrain  $k_{d-in}$  to the value measured in Fig. 2b.

the substrate appear to affect the observed dissociation rate constant for very short DNA strands (Figs. 3b, 4b, and 5b). For this reason, oligonucleotides less than 30 nt in length are not included in the fits.

The linear relationship between the observed dissociation rate constant and the oligonucleotide length suggests that Dda translocates unidirectionally. For unidirectional translocation, the dissociation rate constant is inversely proportional to the length of the DNA.<sup>19</sup> If the helicase were to translocate bidirectionally, the dissociation rate constant would be inversely proportional to the square of the length.<sup>19,20</sup> The data indicate that

Dda translocates unidirectionally at a velocity of  $252 \pm 11$  nt/s. Although these results do not indicate the direction of translocation, these results are consistent with previous results suggesting that Dda translocates in the 5'-to-3' direction.<sup>8-10</sup>

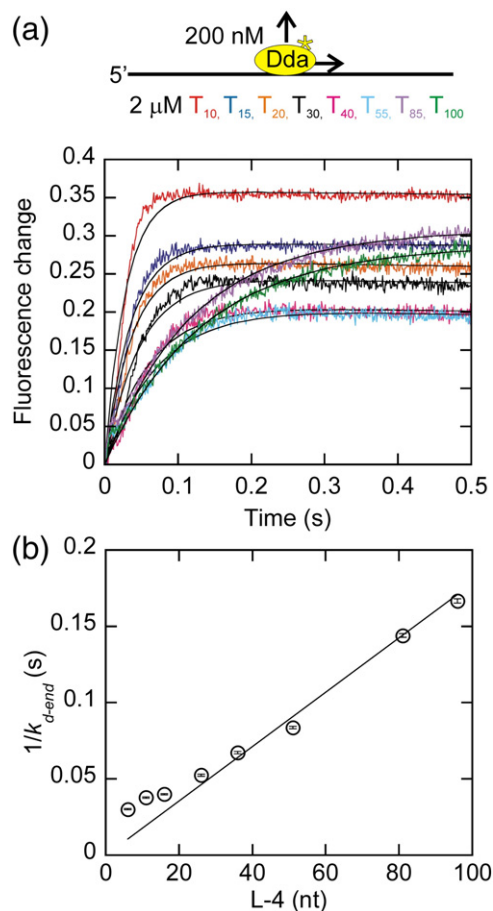


**Fig. 4.** Change in tryptophan fluorescence as a function of oligonucleotide length with homopolymeric oligonucleotides. (a) The change in fluorescence of 200 nM Dda as it dissociates from 2  $\mu$ M (in nucleotides) dT<sub>10</sub>, dT<sub>15</sub>, dT<sub>20</sub>, dT<sub>30</sub>, dT<sub>40</sub>, dT<sub>55</sub>, dT<sub>85</sub>, and dT<sub>100</sub> is plotted. The observed dissociation rate constants, obtained by fitting to a single exponential, were  $35.0 \pm 0.4$  s $^{-1}$ ,  $28.3 \pm 0.3$  s $^{-1}$ ,  $26.8 \pm 0.3$  s $^{-1}$ ,  $22.4 \pm 0.3$  s $^{-1}$ ,  $16.6 \pm 0.2$  s $^{-1}$ ,  $13.7 \pm 0.2$  s $^{-1}$ ,  $8.7 \pm 0.1$  s $^{-1}$ , and  $7.8 \pm 0.1$  s $^{-1}$  for dissociation from dT<sub>10</sub>, dT<sub>15</sub>, dT<sub>20</sub>, dT<sub>30</sub>, dT<sub>40</sub>, dT<sub>55</sub>, dT<sub>85</sub>, and dT<sub>100</sub>, respectively. (b) The inverse of the rate constant for dissociation from the end of the oligonucleotide,  $k_{d-end}$ , which is equal to the observed dissociation rate constant minus the intrinsic dissociation rate constant (Fig. 2b), is plotted versus the length of the substrate, adjusted for binding site size. Only oligonucleotides of at least 30 nt in length are included in the fit. One-half the inverse slope of the resulting line provides a translocation velocity of  $264 \pm 10$  nt/s. The fit was constrained through the origin to constrain  $k_{d-in}$  to the value measured in Fig. 2b.



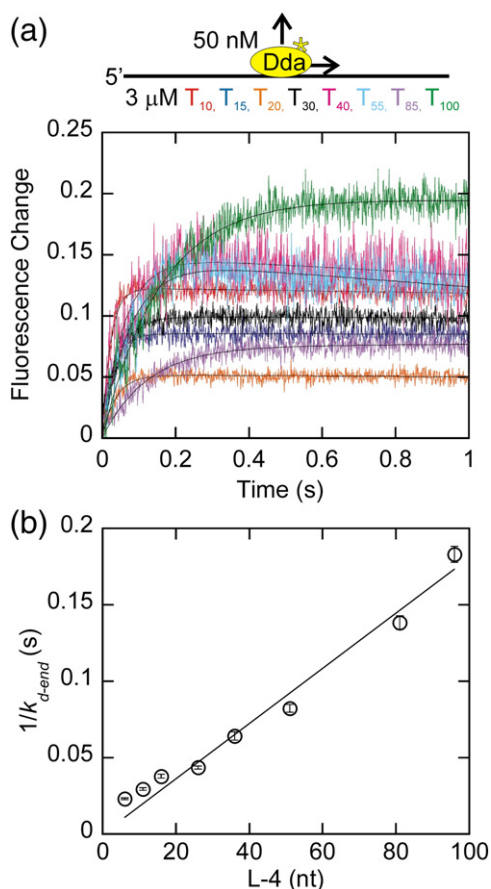


**Fig. 5.** Change in tryptophan fluorescence as a function of oligonucleotide length with homopolymeric oligonucleotides under conditions where the substrate concentration is in vast excess. (a) The change in fluorescence of 50 nM Dda as it dissociates from 3  $\mu$ M (in nucleotides) dT<sub>10</sub>, dT<sub>15</sub>, dT<sub>20</sub>, dT<sub>30</sub>, dT<sub>40</sub>, dT<sub>55</sub>, dT<sub>85</sub>, and dT<sub>100</sub> is plotted. The observed dissociation rate constants obtained by fitting to a single exponential were  $44.1 \pm 1.0$  s<sup>-1</sup>,  $34.7 \pm 1.0$  s<sup>-1</sup>,  $27.2 \pm 0.8$  s<sup>-1</sup>,  $23.8 \pm 0.5$  s<sup>-1</sup>,  $16.4 \pm 0.7$  s<sup>-1</sup>,  $13.0 \pm 0.4$  s<sup>-1</sup>,  $8.1 \pm 0.2$  s<sup>-1</sup>, and  $6.3 \pm 0.2$  s<sup>-1</sup> for dissociation from dT<sub>10</sub>, dT<sub>15</sub>, dT<sub>20</sub>, dT<sub>30</sub>, dT<sub>40</sub>, dT<sub>55</sub>, dT<sub>85</sub>, and dT<sub>100</sub>, respectively. (b) The inverse of the rate constant for dissociation from the end of the oligonucleotide,  $k_{d-end}$ , which is equal to the observed dissociation rate constant minus the intrinsic dissociation rate constant (Fig. 2b), is plotted *versus* the length of the substrate, adjusted for binding site size. Only oligonucleotides of at least 30 nt in length are included in the fit. One-half the inverse slope of the resulting line provides a translocation velocity of  $287 \pm 13$  nt/s. The fit was constrained through the origin to constrain  $k_{d-in}$  to the value measured in Fig. 2b.

### Measurement of the rate constant for Dda dissociation from homopolymeric oligonucleotides

In order to ensure that there are no sequence-dependent effects on the translocation velocity, we performed a similar experiment with homopoly-

meric DNA (Fig. 4). The resulting translocation velocity of  $264 \pm 10$  nt/s is very similar to the velocity obtained with mixed sequence oligonucleotides, indicating that Dda is not sensitive to the sequence of the substrate. As with the mixed sequence oligonucleotides, the relationship between the dissociation rate constant and the DNA length is not linear for oligonucleotides less than 30 nt in length. This could be due to the ends of the DNA affecting the observed dissociation rate. Since dissociation is fastest from short oligonucleotides, any effects due to the ends of the oligonucleotides will have the most impact on the observed dissociation rate from short oligonucleotides. Since the rate constant for dissociation from the end of the oligonucleotide is proportional to the length of the substrate for oligonucleotides of at least 30 nt, only these substrates are included in the fit.

Although the number of Dda binding sites is in excess of the Dda concentration in these experiments, more than one Dda molecule can be bound to the ssDNA at the concentrations in these experiments. Thus, the concentration of DNA was increased to decrease the likelihood of multiple enzymes binding to each DNA substrate. With a 10-fold excess of enzyme binding sites, the translocation velocity is  $287 \pm 13$  nt/s (Fig. 5b) using the data from oligonucleotides of at least 30 nt in length. This is in close agreement with the translocation velocities obtained earlier, indicating that the multiple Dda molecules were not influencing each other in the translocation experiments.

### Measurement of the velocity of Dda translocation on fluorescein-labeled oligonucleotides

We further investigated the ability of Dda to translocate in a unidirectional manner using a fluorescence assay developed by Dillingham *et al.*<sup>20</sup> Dda was pre-incubated with 3'-fluorescein-labeled oligonucleotides. Upon mixing with ATP, an initial decrease in fluorescence was followed by an increase (Fig. 6a). The initial decrease was interpreted to be the result of Dda translocation toward the fluorophore. The subsequent increase in fluorescence most likely results from Dda translocating off the end of the oligonucleotide. Re-initiation of translocation was prevented by the addition of poly(dT). The time to maximal fluorescence quenching is proportional to the length of the oligonucleotide, indicating that the initial decrease in fluorescence corresponds to translocation (Fig. 6b). The inverse of the slope of the line is  $266 \pm 37$  nt/s, which is consistent with the translocation velocity determined from the dissociation experiments. The average translocation velocity obtained for Dda from the data in Figs. 3–6 is  $267 \pm 15$  nt/s. This is nearly identical

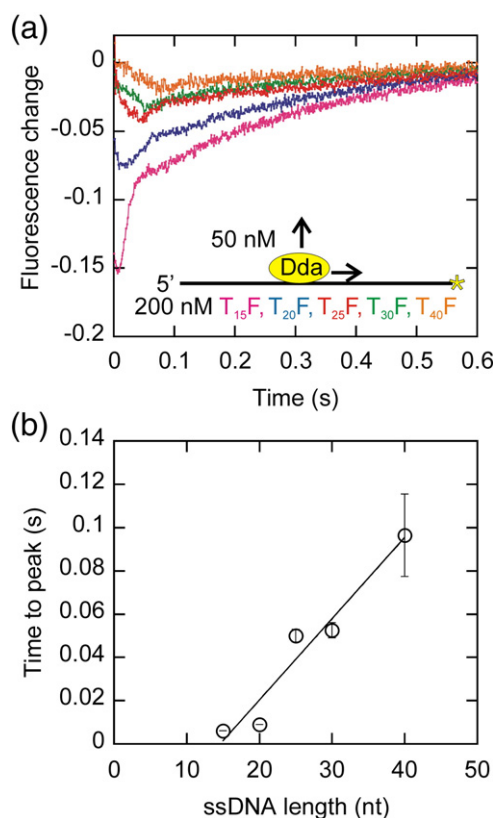


**Fig. 6.** Translocation of Dda along fluorescein-labeled oligonucleotides of various lengths. (a) The change in the fluorescence of 3'-fluorescein-labeled oligonucleotides of varying length was monitored after a 515-nm-cutoff filter in the presence of ATP. The initial decrease in fluorescence was determined to correspond to the translocation of Dda. (b) The time to the maximal fluorescence change is plotted versus the length of the oligonucleotide. The translocation velocity was determined to be  $266 \pm 37$  nt/s by the inverse slope of a linear fit.

to the published unwinding velocity for Dda,  $273 \pm 43$  bp/s.<sup>13,18</sup> Since the translocation velocity,  $V_{\text{trans}}$ , is the same as the published unwinding velocity,  $V_{\text{unw}}$ , Dda is an active helicase using the practical definition recently put forth by Manosas *et al.*<sup>5</sup>

### Dda unwinding is not affected by the GC content of the duplex

Active versus passive helicase mechanisms can be evaluated by comparing the velocity of unwinding of substrates with increasing GC content. The velocities for unwinding by passive helicases are more sensitive to increasing GC content than those by active helicases. The velocity of unwinding by Dda of a 16-bp duplexes of varying GC content was investigated in order to determine whether unwinding by Dda is affected by the stability of the

duplex. Unwinding reactions were performed at 25 °C (Fig. 7a and b) and 20 °C (Fig. 7c and d). When the GC content of the duplex is increased from 50% to 100%, a noticeable increase in the lag phase occurs, and the number of steps required to unwind the substrate increases from 2 to 4 (Fig. 7b and d). The increased number of steps needed to melt the duplex results from the increased stability of the high GC substrates relative to the low GC substrates. For each substrate, the data were fit to an  $n$ -step sequential mechanism (Scheme 1),<sup>21</sup> with the minimum number of steps ( $n$ ) required to provide a fit of the data. The resulting  $n$  values were 2 for the 50% GC substrate, 3 for the 69% and 81% GC substrates, and 4 for the 100% GC substrate. Although the number of steps required to unwind the duplex increases when the stability of the duplex increases,  $V_{\text{unw}}$  remains relatively constant (Table 1) at both 20 °C and 25 °C. If Dda unwinding was affected by the GC content of the duplex, increasing GC content would result in a decrease in the unwinding velocity, which was not observed. This indicates that Dda is not affected by the GC content of the duplex. Table 2 shows the translocation and unwinding velocities obtained under various conditions. The average translocation and unwinding velocities are nearly identical, also indicating that Dda is an active helicase.

The substrate containing 100% GC in the duplex exhibited an additional phase in the unwinding curve. The unusual peak in the reaction progress curve that appears at around 50 ms (Fig. 7b, triangles) indicates formation of an intermediate. A similar intermediate was previously described for unwinding of substrates containing 24 and 28 bp but not for substrates containing 16 or 20 bp.<sup>18</sup> The intermediate was interpreted to be the result of several fast steps in the unwinding reaction followed by a slow rate-limiting step. The intermediate only appeared for those substrates that resulted in lag phases requiring more than three kinetic steps. The 16- and 20-bp substrates described previously required only three kinetic steps to fit the lag phase because these substrates did not have relatively high GC content. In the current report, three of the substrates used here result in unwinding curves that can be described by kinetic mechanisms of two steps (50% GC) or three steps (69% GC and 81% GC). However, the unwinding curve for the substrate containing 100% GC content is best described by a model that includes four kinetic steps. Hence, the appearance of the intermediate is consistent with the increased number of steps needed to unwind the substrate containing 100% GC content, just as reported previously for unwinding of 24- and 28-bp duplexes.<sup>18</sup> The increase in number of steps needed for unwinding is a result of the increased stability of the duplex, which is determined by the GC content and the length of the duplex.

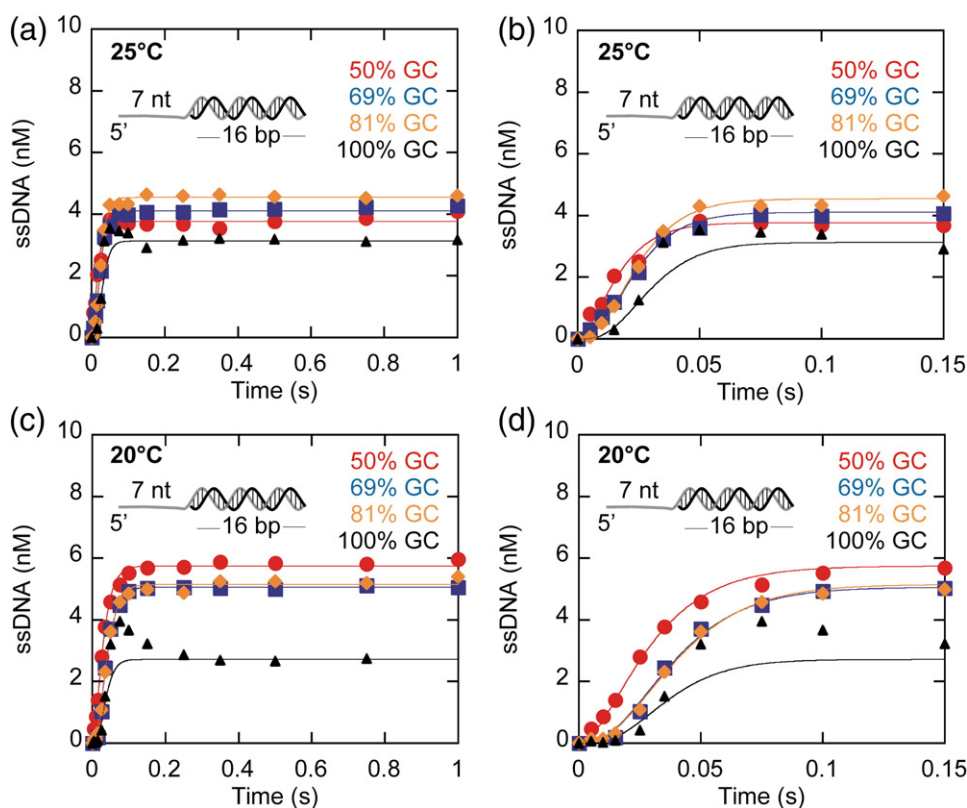


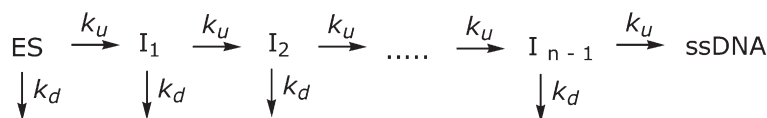
**Fig. 7.** Unwinding of 16-bp duplexes of varying stability by Dda. (a and b) Unwinding of 10 nM partial duplex substrates of varying stability by 100 nM Dda at 25 °C. Data were fit using KinTek Explorer<sup>56</sup> to Scheme 1. The velocities of unwinding were  $205 \pm 26$  bp/s,  $232 \pm 16$  bp/s,  $231 \pm 10$  bp/s, and  $234 \pm 27$  bp/s for unwinding of 50%, 69%, 81%, and 100% GC substrates, respectively. (c and d) Unwinding of the same substrates at 20 °C. The velocities for unwinding were  $143 \pm 8$  bp/s,  $151 \pm 9$  bp/s,  $148 \pm 8$  bp/s, and  $185 \pm 21$  s<sup>-1</sup> for unwinding of 50%, 69%, 81%, and 100% GC substrates, respectively.

### Single-molecule unwinding and translocation

Single-molecule helicase assays were conducted with magnetic tweezers using a 1.2-kb DNA hairpin specifically attached between a glass surface and a micrometer-sized magnetic bead<sup>22</sup> as a substrate. The hairpin contains a dsDNA stem of 1139 bp, ending with a four-T loop on one side. At the other end is a fork; one arm of the fork is a 5'-biotinylated 76-base ssDNA. The other contains 10 nt of ssDNA and 150 bases of duplex DNA labeled with digoxigenin on the 3'-end. The magnetic field gradient generated by two permanent magnets produces a strong vertical force whose magnitude is controlled by adjusting the magnet's position relative to the sample. Dda

unwinding of the fork junction results in a gradual increase in the molecule extension, corresponding to the gain of two bases for each base pair unwound. The helicase concentration was very low (about 250 pM) so that each unwinding event is the result of a single enzyme action.

In the presence of saturating ATP, unwinding bursts are observed (Fig. 8a–c). They all start with an unwinding phase of a few hundred base pairs. After the unwinding phase, two scenarios are possible: a quasi-instantaneous rezipping of the hairpin due to the helicase dissociation (Fig. 8a) or a slow rezipping, with a velocity comparable to the unwinding velocity (Fig. 8b). Combinations of these different phases occurred frequently. This is dependent on the force used to pull the hairpin; slow rezipping is



**Scheme 1.**  $n$ -step sequential mechanism for fitting unwinding data.

**Table 1.** The unwinding velocity is insensitive to the GC content of the duplex

GC (%)	$n^a$	$L_0^b$ (bp)	at 25 °C		at 20 °C	
			$k_{un}$ (s <sup>-1</sup> )	$V_{un}$ (bp/s)	$k_{un}$ (s <sup>-1</sup> )	$V_{un}$ (bp/s)
50	2	10	68.2	205	47.7	143
69	3	8 <sup>18</sup>	87.0	232	56.7	151
81	3	8	86.6	231	55.4	148
100	4	6	93.5	234	74.0	185

<sup>a</sup>  $n$  is the number of steps in the unwinding mechanism (Scheme 1).

<sup>b</sup>  $L_0$  is the number of base pairs that spontaneously melt.<sup>18</sup>

absent at 5 pN, and at forces higher than 8 pN, slow rezipping constitutes about 10% of the total events observed. The unwinding speed is uniform, and unwinding events are often interrupted by partial rezipping corresponding to the helicase slipping backwards by tens to hundreds of base pairs as evidenced by a rapid re-annealing of the hairpin fork (Fig. 8c). The helicase resumes unwinding after such slippage events. Slippages are observed even at very low helicase concentrations, implying that the same enzyme is involved in both events, since dissociation followed by rapid binding is not possible at these low concentrations. During this slippage, the enzyme keeps a contact with DNA since it can regain its grip on ssDNA and resume unwinding. Such behavior is easier to understand for a hexameric enzyme such as the T7 gp4 helicase that encircles ssDNA<sup>23</sup> than for a monomeric enzyme such as Dda, especially since other non-hexameric helicases such as UvrD and RecQ rarely slip during unwinding.<sup>24</sup> During its course of unwinding, Dda may also interact with the displaced DNA strand, resulting in a strand-switching event, characterized by translocation reducing the hairpin re-annealing as observed previously in UvrD.<sup>24</sup> The hairpin fork then does not re-anneal instantaneously but refolds in the wake of the translocating enzyme, with a rate equal to the translocation speed of the helicase (Fig. 8b). These events enable us to study Dda translocation in addition to its unwinding activity. In all these events, the translocation speed is nearly equal to the unwinding speed.

An important question that arises is whether the helicase activity is assisted by force applied to the hairpin fork. For a passive helicase, the unwinding speed would increase with the applied force because the force effectively lowers the energy barrier for the helicase to open the double helix. In the case of Dda, we find that the unwinding speed is insensitive to the force applied. For forces ranging from 5 to 13 pN, the unwinding speed remains close to 250 bp/s, within experimental and statistical errors (Fig. 8f), indicating that Dda is an active helicase. As

in ensemble experiments, the ratio between the unwinding and the translocation velocities remains close to 1 (considering experimental errors) for the whole range of forces studied (Fig. 8e). The apparently lower unwinding velocity might be a systematic effect of undetected small slippage events and the substantial error in the translocation rate. Dda is not a very processive helicase, and at the single-molecule level, the different unwinding bursts of Dda have an exponentially distributed processivity. Interestingly, just like the unwinding speed, the processivity is insensitive to the force used to pull the hairpin, as shown in Fig. 8d. The above observations certify that Dda falls in the class of the so-called “active” helicases.<sup>5</sup>

## Discussion

The mechanisms for helicase-catalyzed DNA unwinding are beginning to be understood at the molecular level. One of the ways that helicases have been characterized is in terms of active *versus* passive mechanisms. An active helicase interacts with the DNA, resulting in destabilization of the duplex. A passive helicase traps localized melting that occurs through thermal fluctuations.<sup>4</sup> Most helicases are not completely active or passive but display activity between these two extremes. One way to quantify this property is to specify the level of destabilizing energy involved in the interaction of the helicase with the DNA fork. A recent report provides a practical guide for distinguishing between active and passive helicases.<sup>5</sup>  $V_{trans}$  on ssDNA can be measured via several approaches including bulk fluorescence methods<sup>20,25–29</sup> and single-molecule methods.<sup>24,30–37</sup> This velocity can then be compared to the velocity of unwinding dsDNA ( $V_{un}$ ). Those helicases that have a ratio of  $V_{un}/V_{trans}$  that is close to 1 are considered to be highly active. Helicases that exhibit a low ratio are considered passive. The ratio that corresponds to an active helicase has been suggested as  $> 0.25$ , based on data from a few helicases for which velocities are available and on a theoretical analysis.<sup>5,38</sup> For example, *Escherichia coli* RecQ is active ( $V_{un}/V_{trans} \sim 0.9$ ), and T4 gp41 is passive ( $V_{un}/V_{trans} \sim 0.08$ ).<sup>5</sup> Helicases need not be completely

**Table 2.** The unwinding and translocation velocities are the same for Dda

Translocation data source	$V_{trans}$ (nt/s)	Unwinding data source	$V_{un}$ (bp/s)
Fig. 3	252 ± 11	Ref. 18	304 ± 50
Fig. 4	264 ± 10	Ref. 13	242 ± 25
Fig. 5	287 ± 13	Fig. 7	225 ± 14
Fig. 6	266 ± 37		
Average	267 ± 15	Average	257 ± 42



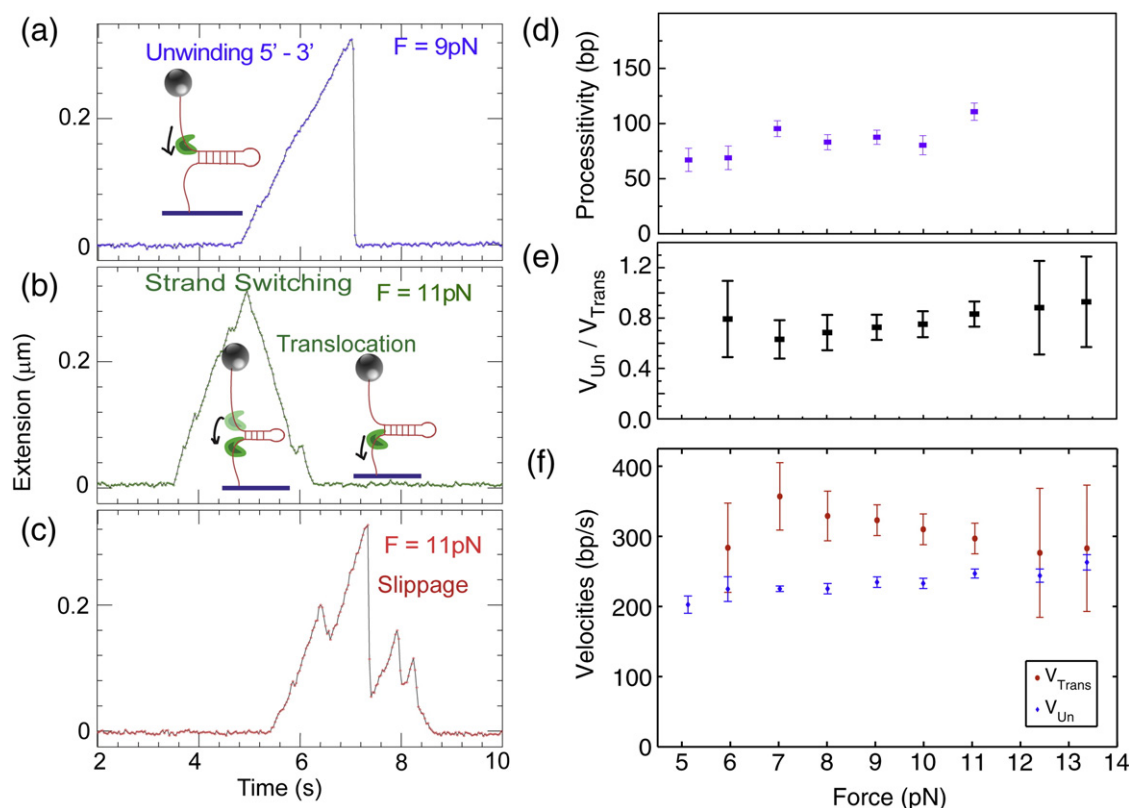


**Fig. 8.** Single-molecule unwinding and translocation. One end of a DNA hairpin substrate was attached to a glass coverslip, and the other end was attached to a magnetic bead. Magnets were used to pull the bead at a constant force. The force applied was low enough to prevent mechanical unzipping (below 15 pN). This geometry enabled us to follow the enzyme dynamics as a function of the applied force. (a) A typical unwinding event presenting a regular speed of unwinding by Dda in the 5'-to-3' direction, followed by enzyme dissociation and rapid re-annealing of the hairpin (at 9 pN, 1 bp  $\sim$  0.9 nm). (b) Dda, during its course of unwinding, can sometimes switch strands and just translocate in the 5'-to-3' direction. While the helicase is unwinding the 1139-bp hairpin, its extension increases. Dda switches strands after unwinding about 300 bp (at 11 pN, 1 bp unwound  $\sim$  0.98 nm extension increase). The helicase then translocates and the hairpin re-zips in its wake, at a rate limited by the translocation speed of the enzyme. Note that the rate of decrease in extension (translocation velocity) is equivalent to the rate of increase of extension (unwinding velocity). (c) An event demonstrating repeated unwinding due to slippages. In our experimental conditions, slippages occurred frequently. Dda processivity (d), unwinding velocity (f), and translocation velocity (f) *versus* applied force, measured in single-molecule unwinding assays. (e) Dependence on force of the ratio of the unwinding speed to the translocation speed. Notice that the translocation velocity is obtained whenever Dda switches strands; as those events are short and sparse at low force, the error bars associated are rather large, and it was not possible to measure this parameter at 5 pN.

active or passive; for example, for a helicase with  $V_{un}/V_{trans}=0.25$ , melting of dsDNA may be partially rate limiting, while for a helicase with  $V_{un}/V_{trans}=1$ , the helicase physically separates the duplex and a component of the ATPase cycle or translocation is rate limiting.

The average velocity of Dda translocation on ssDNA ( $267 \pm 15$  nt/s) was calculated by comparing the rate constant for Dda dissociation from oligonucleotides of various lengths to that from circular DNA. The translocation velocity was also confirmed by measuring the time to the maximal decrease in fluorescence of 3'-fluorescein-labeled oligonucleotides and by single-molecule techniques. The velocity of translocation on ssDNA by Dda is essentially

the same as the reported velocity of unwinding<sup>13,18</sup> and that measured in Fig. 7 (average is  $257 \pm 42$  bp/s). This velocity is also comparable to that of unwinding by single molecules of Dda (Fig. 8f). For Dda, the ratio of  $V_{un}/V_{trans}$  is 0.96. The unwinding and translocation velocities are nearly identical and well within the experimental error, making this essentially a "perfectly active" helicase. The close match between the unwinding and translocation velocities indicates that unwinding of dsDNA by Dda is limited by the rate of translocation on ssDNA. These results are consistent with previous reports showing that when multiple Dda molecules are bound to a single unwinding substrate, the trailing molecules and the leading molecules move at similar rates,<sup>13</sup> which means

that DNA unwinding due to the lead molecule occurs at the same rate as translocation on ssDNA of the trailing molecules. These results suggest that the rate-limiting step for unwinding by Dda is a component of translocation, not of unwinding, per se.

Other helicases with ratios that approach 1 are RecQ and UvrD. In the case of UvrD, the enzyme forms oligomeric species during unwinding, making direct comparisons between translocation and unzipping less straightforward. Wu *et al.* found that RecBC can simultaneously translocate in the 5'-to-3' direction at the same rate as the 3'-to-5' direction.<sup>37</sup> However, the velocity of unwinding under the same conditions is slower than translocation on one strand ( $V_{\text{un}}/V_{\text{trans}} \sim 0.39$ ) or on both strands ( $V_{\text{un}}/V_{\text{trans}} \sim 0.54$ ).<sup>37</sup>

The fact that some helicases translocate on ssDNA much faster than they unzip dsDNA indicates that helicase mechanisms can be much more complex than acting simply as "snow plows". The presence of a complementary strand of NA slows down a passive helicase, resulting in a significantly slower unwinding velocity than translocation velocity. For example, hexameric helicase T4 gp41 unwinds dsDNA at the relatively slow velocity of  $\sim 30$  bp/s when acting alone.<sup>33,39</sup> However, translocation on ssDNA occurs at  $\sim 400$  nt/s,<sup>33</sup> which is close to the rate of T4 DNA replication. The rate of gp41 is enhanced by more than 10-fold when coupled to the T4 polymerase *in vitro*.<sup>40</sup> Therefore, unwinding and translocation are similar, when the helicase is coupled to the polymerase. The T7 polymerase interacts with T7 gene 4 helicase, greatly enhancing the unwinding velocity. T7 gene 4 translocates on ssDNA at 130 nt/s<sup>41</sup> but unwinds DNA at 10–50 bp/s.<sup>42</sup> When coupled to the T7 polymerase, gene 4 helicase unwinds DNA at 90–130 bp/s.<sup>43</sup> Therefore, some helicases require a second motor protein in order to fully utilize translocation activity for DNA unwinding activity. Dda does not appear to require accessory proteins to unwind dsDNA at an equivalent velocity to that at which it translocates on ssDNA.

An alternative way to distinguish active *versus* passive helicases is to measure unwinding with substrates of different GC content. Since an AT base pair is about half as stable as a GC base pair,<sup>5</sup> the unwinding velocity of a passive helicase will decrease with increasing GC content of the duplex. However, an active helicase will be unaffected. RecQ, an active helicase, is somewhat sensitive to the GC content of the duplex with the  $V_{\text{un}}^{\text{GC}}/V_{\text{un}}^{\text{AT}} \sim 0.7$ .<sup>5</sup> Donmez *et al.* have shown that the velocity of unwinding GC-rich NA is 6-fold less than AT-rich NA for T7 helicase and NS3/4a on RNA. The difference decreases to 3-fold for NS3/4a on DNA substrates and for NS3h on both DNA and RNA.<sup>42</sup> Dda is the first helicase that has been shown to have both  $V_{\text{un}}/V_{\text{trans}} \sim 1$  and  $V_{\text{un}}^{\text{GC}}/V_{\text{un}}^{\text{AT}} \sim 1$  (Table 2), further emphasizing its characteristics as a "perfectly" active helicase.

The fact that Dda is insensitive to the GC content is consistent with a short stepsize that occurs with high force, similar to the chromatin remodeling enzyme RSC.<sup>44</sup> Force production is consistent with a role in which Dda removes proteins from the DNA.<sup>10,16,45–47</sup> Numerous helicases that displace other proteins from DNA have been found. Rrm3 removes proteins bound to DNA *in vivo* during DNA replication in yeast.<sup>48</sup> Rep helicase was found to push DnaB helicase during replication in *E. coli*.<sup>49</sup> Srs2 regulates recombination by displacing recombinase filaments,<sup>50</sup> and Pif1 displaces telomerase to regulate telomere length.<sup>51</sup> In some cases, such as with Srs2, a specific protein–protein interaction between the helicase and the displaced protein induces allosteric changes in the protein that lead to its dissociation from DNA.<sup>50</sup> Dda can displace streptavidin from biotin-labeled DNA<sup>10,15</sup> and has been observed to readily displace DNA-binding proteins from its path during translocation and DNA unwinding,<sup>16</sup> suggesting that force production occurs when the enzyme moves.

Single-molecule Dda unwinding events reveal interesting insights into its activity and interaction with the DNA substrate. In addition to the translocation and unwinding velocities obtained from single-molecule experiments being similar to those from ensemble experiments, the  $V_{\text{un}}/V_{\text{trans}}$  ratio is close to 1 and remains constant as the applied force varies, also indicating that Dda is an active helicase. The slippage events provide evidence that Dda keeps a loose contact with its substrate even during a fast re-zipping. This may occur through an interaction with the displaced strand as suggested,<sup>18</sup> which would facilitate the strand switching observed in some single-molecule experiments. Interaction with both strands of the duplex would appear to be advantageous for active helicases.

DNA unwinding requires a step in which the strands are actually separated (melting), as well as a step in which the enzyme moves along the DNA (translocation). It is possible that translocation and unwinding occur concomitantly as a result of movement of the enzyme, but it is also possible that translocation and unwinding occur separately. If the steps are separate, then melting must occur faster, so as to not be rate limiting. Regardless of the specific mechanism, it would appear that the overall rate for unwinding is limited by a step within the ATPase cycle. For example, ATP hydrolysis, dissociation of ADP or  $P_i$ , or a conformational change in the enzyme might limit the overall rate. The rate-limiting step for some helicases such as T7 gene 4 helicase,<sup>52</sup> Rho transcription termination factor,<sup>53</sup> and HCV NS3 helicase<sup>54</sup> has been proposed to occur with release of  $P_i$ .

The fact that Dda separates the duplex in an active manner predicts that protein–NA interactions facilitate melting. Evidence for some interaction with the

displaced strand was provided when an intermediate in the unwinding reaction was discovered.<sup>18</sup> The intermediate was explained as a consequence of a slow step for dissociation of the displaced strand after two to three steps of unwinding. In the current work, we observed a similar intermediate during unwinding of a substrate containing high GC content. The appearance of this intermediate was not observed with substrates that required only two to three steps prior to melting. It was only observed with the high GC content substrate, supporting the conclusion that Dda interacts with both strands, leading to the appearance of the intermediate. The ability of the helicase to switch strands in single-molecule experiments and to re-initiate unwinding after slipping also indicates that there may be an interaction between Dda and the displaced strand. In fact, interaction with the displaced strand may actually slow down a helicase rather than enhance activity. In the case of the Pif1 helicase, a DNA:RNA hybrid is unwound faster than a DNA:DNA hybrid. The mechanism for this preference is not known, but it could be due to specific interactions between Pif1 and RNA that activate the helicase, or it could be due to specific interactions between Pif1 and DNA that slow down the helicase. Hence, interaction with the displaced strand may increase or decrease the overall rate of DNA unwinding, depending on the specific mechanism of a helicase.

Thus far, structural studies have not captured the intermediates revealing the specific molecular mechanism(s) for the melting step in helicase-catalyzed DNA unwinding. Thus, the specific molecular events that occur between a helicase and a duplex DNA remain unknown. The fact that Dda helicase moves along ssDNA at the same velocity as it unwinds dsDNA indicates that when the enzyme encounters the duplex, its forward motion is not impeded. This could be due to specific interactions that occur between the enzyme and the first base pair. Binding interactions between the helicase and the DNA must lower the activation barrier for melting of the duplex.<sup>5</sup> Such interactions might include stacking with amino acid residues or hydrogen bonding with the bases, or perhaps distortion of the duplex through kinking of the DNA. For Dda, these interactions occur in a manner that does not limit the overall rate of forward movement. The conformational changes associated with forward motion might sterically split the duplex, assuming that appropriate amino acid residues are in place. For example, the structures of other superfamily 1B helicases and several DExH helicases contain a hairpin structure referred to as a "pin" that is believed to split the duplex during movement. A combination of binding energy through specific interactions between the enzyme and the base pairs coupled with force production

through translocation is likely responsible for the "perfectly active" mechanism of Dda helicase.

## Materials and Methods

### Materials

Oligonucleotides were purchased from Integrated DNA Technologies and purified as described previously.<sup>15</sup> DNA sequences were as follows: 60mer, 5'-TAACGTATTCAAGATACCTCGTACTCTGTACTGACTGCGATCCGACTGTCCTGCATGATG-3'; 52mer, 5'-T<sub>24</sub>CGCTGATGTCGCCTGGTACGTCGCTGCC-3'; 45mer, 5'-ACCTCGTACTCTGTACTGACTGCGATCCGACTGTCCTGCATGATG-3'; 38mer, 5'-T<sub>8</sub>GTAAGTAACTAGTACCGCTGATGTCGC-3'; 30mer, 5'-CTGACTGCG ATCCGAGTGTCCCTGCATGATG-3'; 15mer, 5'-CTGTCCTGCATGATG-3'; 50% GC, T<sub>7</sub> CGCTATTGTCTACTGG; 69% GC, T<sub>7</sub> CGCTGATGTCGCCTGG; 81% GC, T<sub>7</sub> CGCTGCGGTCGCCTGG; 100% GC, T<sub>7</sub> CGGCGGCGGGGCCCG. A 5'-biotinylated 1139-bp hairpin labeled with several digoxigenins at 3'-end was synthesized as described previously.<sup>55</sup> Dda was overexpressed and purified as described previously.<sup>11</sup>

### Association experiments

All concentrations indicated are after mixing. Dda (200 nM) association with poly(dT) in reaction buffer [25 mM Hepes (pH 7.5), 10 mM KOAc, 0.1 mM ethylenediaminetetraacetic acid, and 2 mM  $\beta$ -mercaptoethanol] was measured by rapidly mixing in a SX.18MV stopped-flow reaction analyzer (Applied Photophysics) at 25 °C. The change in tryptophan fluorescence over time was monitored after a 320-nm-cutoff filter (Newport Optical Filter #FSQ-WG320) with excitation at 280 nm through 1-mm slits.

### Dissociation experiments

Dda was pre-incubated with ssDNA (at the concentrations indicated in the figure legends) in reaction buffer with 10 mM Mg(OAc)<sub>2</sub>. All ssDNA concentrations are in nucleotides so that the number of nucleotides and, therefore, Dda binding sites remains constant as the length of the substrate varies. The reactions were initiated at 25 °C by mixing with heparin (12 mg/ml) in the presence or absence of a saturating concentration of ATP (600  $\mu$ M) (Table S3). The change in tryptophan fluorescence was monitored after a 320-nm-cutoff filter (Newport Optical Filter #FSQ-WG320) with excitation at 280 nm through 1-mm slits (200 nM Dda) or 5-mm slits (50 nM Dda).

### Determination of velocity of translocation of Dda on DNA

For a model where a NA translocase needs to bind to only 1 nt, the number of binding sites is one more than the length of the oligonucleotide (*L*).<sup>28</sup> The length of the

ssDNA is inversely proportional to the rate constant for dissociation from the end of the oligonucleotide ( $k_{d-end}$ ) for an enzyme that translocates unidirectionally on ssDNA.<sup>19</sup> The translocation velocity ( $V_{trans}$ ) can be calculated from these parameters using Eq. (1),<sup>19</sup> where  $k_{d-obs}$  is the observed dissociation rate constant, and  $k_{d-in}$  is the intrinsic rate constant for dissociation from circular DNA.

$$k_{d-obs} - k_{d-in} = k_{d-end} = \frac{2V_{trans}}{L + 1} \quad (1)$$

However, Dda is known to bind 6 nt.<sup>15</sup> Assuming that all 6 nt are required for binding, there are only  $N = L - B + 1 = L - 5$ <sup>28</sup> binding sites ( $N$ ) for binding site size  $B$ . The distance to translocate to reach the end of the oligonucleotide, assuming random binding, is  $(L - 4)/2$ , and  $V_{trans}$  is one-half the inverse slope of a  $1/k_{d-end}$  versus  $L - 4$  plot based on Eq. (2).

$$k_{d-obs} - k_{d-in} = k_{d-end} = \frac{2V_{trans}}{L - 4} \quad (2)$$

### Translocation experiments using fluorescein fluorescence

We pre-incubated 200 nM 3'-fluorescein-labeled oligonucleotides with 50 nM Dda in reaction buffer. The reaction was initiated by mixing with 5 mM ATP, 10 mM Mg(OAc)<sub>2</sub>, and 5  $\mu$ M poly(dT) at 25 °C. The change in fluorescein fluorescence was monitored after a 515-nm-cutoff filter (Newport Optical Filter #51294) with an excitation at 495 nm through 1-mm slits.

### DNA unwinding reactions

Oligonucleotides were radiolabeled as described previously.<sup>11</sup> Unwinding reactions were performed in reaction buffer with 0.1 mg/ml bovine serum albumin using a KinTek rapid chemical quench-flow instrument maintained at 25 °C. All concentrations are after mixing. We incubated 10 nM radiolabeled substrate with 100 nM Dda for 3 min preceding the initiation of the reaction. We added 5 mM ATP, 10 mM Mg(OAc)<sub>2</sub>, 300 nM DNA trap (complementary to the displaced strand), and 5  $\mu$ M poly(dT) (protein trap to prevent rebinding of Dda to the substrate after dissociation) to initiate the reaction. Reactions were quenched with 400 mM ethylenediaminetetraacetic acid, analyzed on a 20% polyacrylamide gel, visualized with a Typhoon Trio phosphorimager (GE Healthcare), and quantified using ImageQuant software (GE Healthcare). Data were fit using KinTek Explorer<sup>56</sup> to Scheme 1. The enzyme-substrate (ES) complex is converted to product in  $n$  identical sequential steps, defined by the rate constant per step,  $k_u$ . At each step, the helicase can also dissociate from the NA with a rate constant of  $k_d$ .  $k_d$  was allowed to float because increasing the GC content of the duplex may increase the dissociation rate by increasing the force opposing the helicase, consistent with the observed greater processivity for translocation than for unwinding. Of the 69% GC substrate, 8 bp are known to spontaneously melt based on previous unwinding studies with methylphosphonate modified

substrates.<sup>18</sup> The velocity of unwinding ( $V_{un}$ ) was calculated using Eq. (3).

$$V_{un} = mk_u \quad (3)$$

The kinetic step size ( $m$ ) is defined by Eq. (4).

$$m = \frac{L - L_0}{n} \quad (4)$$

$L$  is the length of the duplex.  $L_0$  is the number of base pairs that spontaneously melt due to thermal fluctuations and are not unwound by the helicase.<sup>18</sup> The number of steps required for the helicase to unwind the duplex is  $n$ .

### Single-molecule experiments

Streptavidin-coated MyOne (Invitrogen) magnetic beads were pulled by the magnetic tweezers formed by a pair of permanent magnets<sup>55</sup> whose position relative to an antidigoxigenin-coated coverslip was monitored, providing a means to change the force exerted on the hairpin over a range of  $10^{-2}$ –30 pN. The extension of typically 50 molecules was measured using the ring diffraction image of the bead<sup>57</sup> at a temperature of 28 °C by 250 pM Dda in a buffer consisting of 20mM Tris-HCl (pH 7.6), 25 mM NaCl, 3 mM MgCl<sub>2</sub>, 2% bovine serum albumin, 0.5 mM dithiothreitol, and 1 mM ATP. A constant force below the threshold for mechanically unzipping the DNA was maintained. Linear fits of the change in extension over time provided unwinding rates. Translocation velocities were obtained in a similar manner from translocation events. The rate of change in extension of the substrate was converted to base pairs using the force-extension curve of ssDNA of a well-defined length in bases in identical buffer conditions. Sometimes, Dda displaced the digoxigenin from the DNA; therefore, the experiments were repeated several times in order to collect a large number of unwinding and translocation events. The distribution of unwinding/translocation velocity was computed from 250 to 850 events, depending on the conditions, and presented a Gaussian shape. The errors in the unwinding rate were obtained as a sum of the statistical error and the error in the extension of ssDNA. The mean processivity of the helicase was calculated from the distribution of the maximum number of base pairs unwound in each single burst of activity. The histograms of these events were fit to an exponential whose characteristic length leads to the processivity.

### Acknowledgements

We would like to thank Carrie Brown and Clint Langston for technical assistance. This work was supported by National Institutes of Health Grant R01 GM098922 (K.D.R.), National Institutes of Health Grant #P20 RR-16460 from the IDeA Networks of Biomedical Research Excellence Program of the National Center for Research Resources (D.L.M.), Agence Nationale de la Recherche,



Human Frontier Science Program Grant RGP003/2007 (V.C.), the European Research Council Grant "MagRepS"267862 (V.C. and D.B.), the University of Arkansas for Medical Sciences graduate student research fund (A.K.B.), and Award Number UL1RR029884 from the National Center for Research Resources (to C. Lowery).

## Supplementary Data

Supplementary data to this article can be found online at [doi:10.1016/j.jmb.2012.04.007](https://doi.org/10.1016/j.jmb.2012.04.007)

## References

- Dillingham, M. S. (2011). Superfamily I helicases as modular components of DNA-processing machines. *Biochem. Soc. Trans.* **39**, 413–423.
- Bustamante, C., Cheng, W. & Mejia, Y. X. (2011). Revisiting the central dogma one molecule at a time. *Cell*, **144**, 480–497.
- Maher, R. L., Branagan, A. M. & Morrical, S. W. (2011). Coordination of DNA replication and recombination activities in the maintenance of genome stability. *J. Cell. Biochem.* **112**, 2672–2682.
- Lohman, T. M. (1992). *Escherichia coli* DNA helicases: mechanisms of DNA unwinding. *Mol. Microbiol.* **6**, 5–14.
- Manosas, M., Xi, X. G., Bensimon, D. & Croquette, V. (2010). Active and passive mechanisms of helicases. *Nucleic Acids Res.* **38**, 5518–5526.
- Gauss, P., Park, K., Spencer, T. E. & Hacker, K. J. (1994). DNA helicase requirements for DNA replication during bacteriophage T4 infection. *J. Bacteriol.* **176**, 1667–1672.
- Kodadek, T. & Alberts, B. M. (1987). Stimulation of protein-directed strand exchange by a DNA helicase. *Nature*, **326**, 312–314.
- Jongeneel, C. V., Formosa, T. & Alberts, B. M. (1984). Purification and characterization of the bacteriophage T4 dda protein. A DNA helicase that associates with the viral helix-destabilizing protein. *J. Biol. Chem.* **259**, 12925–12932.
- Raney, K. D. & Benkovic, S. J. (1995). Bacteriophage T4 Dda helicase translocates in a unidirectional fashion on single-stranded DNA. *J. Biol. Chem.* **270**, 22236–22242.
- Morris, P. D. & Raney, K. D. (1999). DNA helicases displace streptavidin from biotin-labeled oligonucleotides. *Biochemistry*, **38**, 5164–5171.
- Morris, P. D., Tackett, A. J., Babb, K., Nanduri, B., Chick, C., Scott, J. & Raney, K. D. (2001). Evidence for a functional monomeric form of the bacteriophage T4 Dda helicase. Dda does not form stable oligomeric structures. *J. Biol. Chem.* **276**, 19691–19698.
- Nanduri, B., Byrd, A. K., Eoff, R. L., Tackett, A. J. & Raney, K. D. (2002). Pre-steady-state DNA unwinding by bacteriophage T4 Dda helicase reveals a monomeric molecular motor. *Proc. Natl Acad. Sci. USA*, **99**, 14722–14727.
- Eoff, R. L. & Raney, K. D. (2010). Kinetic mechanism for DNA unwinding by multiple molecules of Dda helicase aligned on DNA. *Biochemistry*, **49**, 4543–4553.
- Byrd, A. K. & Raney, K. D. (2005). Increasing the length of the single-stranded overhang enhances unwinding of duplex DNA by bacteriophage T4 Dda helicase. *Biochemistry*, **44**, 12990–12997.
- Byrd, A. K. & Raney, K. D. (2004). Protein displacement by an assembly of helicase molecules aligned along single-stranded DNA. *Nat. Struct. Mol. Biol.* **11**, 531–538.
- Byrd, A. K. & Raney, K. D. (2006). Displacement of a DNA binding protein by Dda helicase. *Nucleic Acids Res.* **34**, 3020–3029.
- Tackett, A. J., Morris, P. D., Dennis, R., Goodwin, T. E. & Raney, K. D. (2001). Unwinding of unnatural substrates by a DNA helicase. *Biochemistry*, **40**, 543–548.
- Eoff, R. L. & Raney, K. D. (2006). Intermediates revealed in the kinetic mechanism for DNA unwinding by a monomeric helicase. *Nat. Struct. Mol. Biol.* **13**, 242–249.
- Young, M. C., Kuhl, S. B. & von Hippel, P. H. (1994). Kinetic theory of ATP-driven translocases on one-dimensional polymer lattices. *J. Mol. Biol.* **235**, 1436–1446.
- Dillingham, M. S., Wigley, D. B. & Webb, M. R. (2002). Direct measurement of single-stranded DNA translocation by PcrA helicase using the fluorescent base analogue 2-aminopurine. *Biochemistry*, **41**, 643–651.
- Lucius, A. L., Maluf, N. K., Fischer, C. J. & Lohman, T. M. (2003). General methods for analysis of sequential "n-step" kinetic mechanisms: application to single turnover kinetics of helicase-catalyzed DNA unwinding. *Biophys. J.* **85**, 2224–2239.
- Lionnet, T., Dawid, A., Bigot, S., Barre, F. X., Saleh, O. A., Heslot, F. *et al.* (2006). DNA mechanics as a tool to probe helicase and translocase activity. *Nucleic Acids Res.* **34**, 4232–4244.
- Sun, B., Johnson, D. S., Patel, G., Smith, B. Y., Pandey, M., Patel, S. S. & Wang, M. D. (2011). ATP-induced helicase slippage reveals highly coordinated subunits. *Nature*, **478**, 132–135.
- Dessinges, M. N., Lionnet, T., Xi, X. G., Bensimon, D. & Croquette, V. (2004). Single-molecule assay reveals strand switching and enhanced processivity of UvrD. *Proc. Natl Acad. Sci. USA*, **101**, 6439–6444.
- Dillingham, M. S., Wigley, D. B. & Webb, M. R. (2000). Demonstration of unidirectional single-stranded DNA translocation by PcrA helicase: measurement of step size and translocation speed. *Biochemistry*, **39**, 205–212.
- Tomko, E. J., Fischer, C. J., Niedziela-Majka, A. & Lohman, T. M. (2007). A nonuniform stepping mechanism for *E. coli* UvrD monomer translocation along single-stranded DNA. *Mol. Cell*, **26**, 335–347.
- Tomko, E. J., Ja, H., Park, J., Maluf, N. K., Ha, T. & Lohman, T. M. (2010). 5'-Single-stranded/duplex DNA junctions are loading sites for *E. coli* UvrD translocases. *EMBO J.* **29**, 3826–3839.
- Rajagopal, V., Gurjar, M., Levin, M. K. & Patel, S. S. (2010). The protease domain increases the translocation stepping efficiency of the hepatitis C virus NS3-4A helicase. *J. Biol. Chem.* **285**, 17821–17832.

29. Matlock, D. L., Yeruva, L., Byrd, A. K., Mackintosh, S. G., Langston, C., Brown, C. *et al.* (2010). Investigation of translocation, DNA unwinding, and protein displacement by NS3h, the helicase domain from the hepatitis C virus helicase. *Biochemistry*, **49**, 2097–2109.
30. Bianco, P. R., Brewer, L. R., Corzett, M., Balhorn, R., Yeh, Y., Kowalczykowski, S. C. & Baskin, R. J. (2001). Processive translocation and DNA unwinding by individual RecBCD enzyme molecules. *Nature*, **409**, 374–378.
31. Myong, S., Rasnik, I., Joo, C., Lohman, T. M. & Ha, T. (2005). Repetitive shuttling of a motor protein on DNA. *Nature*, **437**, 1321–1325.
32. Johnson, D. S., Bai, L., Smith, B. Y., Patel, S. S. & Wang, M. D. (2007). Single-molecule studies reveal dynamics of DNA unwinding by the ring-shaped T7 helicase. *Cell*, **129**, 1299–1309.
33. Lionnet, T., Spiering, M. M., Benkovic, S. J., Bensimon, D. & Croquette, V. (2007). Real-time observation of bacteriophage T4 gp41 helicase reveals an unwinding mechanism. *Proc. Natl Acad. Sci. USA*, **104**, 19790–19795.
34. Spies, M., Amitani, I., Baskin, R. J. & Kowalczykowski, S. C. (2007). RecBCD enzyme switches lead motor subunits in response to  $\chi$  recognition. *Cell*, **131**, 694–705.
35. Myong, S., Cui, S., Cornish, P. V., Kirchhofer, A., Gack, M. U., Jung, J. U. *et al.* (2009). Cytosolic viral sensor RIG-I is a 5'-triphosphate-dependent translocase on double-stranded RNA. *Science*, **323**, 1070–1074.
36. Park, J., Myong, S., Niedziela-Majka, A., Lee, K. S., Yu, J., Lohman, T. M. & Ha, T. (2010). PcrA helicase dismantles RecA filaments by reeling in DNA in uniform steps. *Cell*, **142**, 544–555.
37. Wu, C. G., Bradford, C. & Lohman, T. M. (2010). *Escherichia coli* RecBC helicase has two translocase activities controlled by a single ATPase motor. *Nat. Struct. Mol. Biol.* **17**, 1210–1217.
38. Betterton, M. D. & Julicher, F. (2005). Opening of nucleic-acid double strands by helicases: active *versus* passive opening. *Phys. Rev. E: Stat., Nonlinear, Soft Matter Phys.* **71**, 011904.
39. Raney, K. D., Carver, T. E. & Benkovic, S. J. (1996). Stoichiometry and DNA unwinding by the bacteriophage T4 41:59 helicase. *J. Biol. Chem.* **271**, 14074–14081.
40. Dong, F., Weitzel, S. E. & von Hippel, P. H. (1996). A coupled complex of T4 DNA replication helicase (gp41) and polymerase (gp43) can perform rapid and processive DNA strand-displacement synthesis. *Proc. Natl Acad. Sci. USA*, **93**, 14456–14461.
41. Kim, D. E., Narayan, M. & Patel, S. S. (2002). T7 DNA helicase: a molecular motor that processively and unidirectionally translocates along single-stranded DNA. *J. Mol. Biol.* **321**, 807–819.
42. Donmez, I., Rajagopal, V., Jeong, Y. J. & Patel, S. S. (2007). Nucleic acid unwinding by hepatitis C virus and bacteriophage T7 helicases is sensitive to base pair stability. *J. Biol. Chem.* **282**, 21116–21123.
43. Stano, N. M., Jeong, Y. J., Donmez, I., Tummalaipalli, P., Levin, M. K. & Patel, S. S. (2005). DNA synthesis provides the driving force to accelerate DNA unwinding by a helicase. *Nature*, **435**, 370–373.
44. Sirinakos, G., Clapier, C. R., Gao, Y., Viswanathan, R., Cairns, B. R. & Zhang, Y. (2011). The RSC chromatin remodelling ATPase translocates DNA with high force and small step size. *EMBO J.* **30**, 2364–2372.
45. Bedinger, P., Hochstrasser, M., Victor Jongeneel, C. & Alberts, B. M. (1983). Properties of the T4 bacteriophage DNA replication apparatus: the T4 *dda* DNA helicase is required to pass a bound RNA polymerase molecule. *Cell*, **34**, 115–123.
46. Bedrosian, C. L. & Bastia, D. (1991). *Escherichia coli* replication terminator protein impedes simian virus 40 (SV40) DNA replication fork movement and SV40 large tumor antigen helicase activity *in vitro* at a prokaryotic terminus sequence. *Proc. Natl Acad. Sci. USA*, **88**, 2618–2622.
47. Yancey-Wrona, J. E. & Matson, S. W. (1992). Bound Lac repressor protein differentially inhibits the unwinding reactions catalyzed by DNA helicases. *Nucleic Acids Res.* **20**, 6713–6721.
48. Azvolinsky, A. S., Dunaway, S., Torres, J. Z., Bessler, J. B. & Zakian, V. A. (2006). The *S. cerevisiae* Rrm3p DNA helicase moves with the replication fork and affects replication of all yeast chromosomes. *Genes Dev.* **20**, 3104–3116.
49. Guy, C. P., Atkinson, J., Gupta, M. K., Mahdi, A., Gwynn, E. J., Rudolph, C. J. *et al.* (2009). Rep provides a second motor at the replisome to promote duplication of protein-bound DNA. *Mol. Cell*, **36**, 654–666.
50. Antony, E., Tomko, Q., Xiao, L., Krejci, L., Lohman, T. M. & Ellengerger, T. (2009). Srs2 disassembles Rad51 filaments by a protein–protein interaction triggering ATP turnover and dissociation of Rad51 from DNA. *Mol. Cell*, **35**, 105–115.
51. Boule, J. B., Vega, L. R. & Zakian, V. A. (2005). The yeast Pif1p helicase removes telomerase from telomeric DNA. *Nature*, **438**, 57–61.
52. Liao, J. C., Jeong, Y. J., Kim, D. E., Patel, S. S. & Oster, G. (2005). Mechanochemistry of T7 DNA helicase. *J. Mol. Biol.* **350**, 452–475.
53. Adelman, J. L., Jeong, Y. J., Liao, J. C., Patel, G., Kim, D. E., Oster, G. & Patel, S. S. (2006). Mechanochemistry of transcription termination factor Rho. *Mol. Cell*, **22**, 611–621.
54. Wang, Q., Arnold, J. J., Uchida, A., Raney, K. D. & Cameron, C. E. (2010). Phosphate release contributes to the rate-limiting step for unwinding by an RNA helicase. *Nucleic Acids Res.* **38**, 1312–1324.
55. Manos, M., Spiering, M. M., Zhuang, Z., Benkovic, S. J. & Croquette, V. (2009). Coupling DNA unwinding activity with primer synthesis in the bacteriophage T4 primosome. *Nat. Chem. Biol.* **5**, 904–912.
56. Johnson, K. A., Simpson, Z. B. & Blom, T. (2009). Global Kinetic Explorer: a new computer program for dynamic simulation and fitting of kinetic data. *Anal. Biochem.* **387**, 20–29.
57. Gosse, C. & Croquette, V. (2002). Magnetic tweezers: micromanipulation and force measurement at the molecular level. *Biophys. J.* **82**, 3314–3329.